Profiles of Steady-State Suction Stress in Unsaturated Soils

Ning Lu, M.ASCE,[1] and D. V. Griffiths, F.ASCE[2]

Abstract: Application of the effective stress principle in unsaturated geotechnical engineering problems often requires explicit knowledge of the stress acting on the soil skeleton due to suction pore water pressure. This stress is defined herein as the suction stress. A theoretical formulation of suction stress profiles, based on the soil water characteristics curve, the soil permeability characteristic curve, and previous shear strength experimental verification, is developed. The theory provides a general quantitative way to calculate vertical suction stress profiles in various unsaturated soils under steady flow rate in the form of infiltration or evaporation.

DOI: 10.1061/(ASCE)1090-0241(2004)130:10(1063)

CE Database subject headings: Soil suction; Stress; Unsaturated soils; Steady flow; Pore water pressure.

Introduction

Since the development of the principle of effective stress by Terzaghi (1925, 1943), the effective stress concept has been widely used in soil mechanics problems, particularly under saturated soil conditions. This stress has been shown to play the major role in a soil's ability or to resist external stress or load under static or dynamic and drained or undrained conditions.

The power of using effective stress in geotechnical analysis lies in its fundamental contribution to the mechanical properties of soil. Although the effective stress cannot be measured directly, total stress, in the form of externally applied loads or self-weight is usually known, and the pore pressure in saturated soil can usually be measured.

In principle, the effective stress principle can be applied to unsaturated soils (e.g., Bishop 1959; Blight 1961; Donald 1961). In reality, two practical difficulties hinder the direct application of the effective stress principle in unsaturated soils. First, the pore pressure is tensional and is not as easily measured or calculated as when soil is saturated. This limitation has been alleviated to some extent in the past 2 decades or so owing to advancements in soil suction measurement and theories in unsaturated soil hydrology. For example, a tensiometer can be used to measure soil suction or matric suction $(u_a - u_w)$ up to 100 kPa, which is important for soil water retention in sandy soil. A thermo-psychrometer has shown to be accurate for soil suctions ranging from 100 to 8,000 kPa, which can be an important suction range for water retention in silty soil. Nevertheless, all the current techniques are limited to certain suction ranges and are subjected to many environmental limitations such as temperature and humidity. Improved soil suction measurement techniques for different types of soils are still needed, and to date no single technique has been developed that can be reliably used to measure suctions in all soils ranging from sand to clay. The second difficulty lies in the fact that, in contrast to saturated soil, not all of the pore water pressure contributes to effective stress. It is well documented that a reduced proportion of the pore water pressure contributes to effective stress, which in this paper will be referred to as the suction stress.

In many unsaturated geotechnical engineering problems such as retaining walls, slope stability, and landfill cap design (e.g., Krahn et al. 1989; Rahardjo and Leong 1997) the profile of effective stress is an important quantity for assessing the integrity of these structures. Thus knowledge of the profile of suction stress becomes important because it directly influences the effective stress. By applying current theories relating to suction, this paper focuses on the development of a general theory to predict profiles of suction stress in unsaturated soils, taking full account of soil type and evaporative/infiltrative conditions. The theory developed will also be amenable to implementation in other analysis tools, such as the finite element method, as applied to practical geotechnical problems involving unsaturated soils.

Coefficient of Effective Stress χ

The relationship between the pore water pressure and the suction stress depends on the degree of soil saturation. It is generally assumed that when a soil is saturated, the pore water pressure is compressive and equals the difference between the total and effective stress. When a soil is essentially dry, however, the remaining water in the voids may sustain highly tensional pore pressures, however, its influence on effective stress is negligible, and total and effective stress are taken to be equal. To account for this range of behavior, Terzaghi's effective stress principle, modified to account for unsaturated soils, can be written in the following form (Bishop 1959):

$$\sigma' = (\sigma - u_a) + \chi(u_a - u_w) \tag{1}$$

where σ'=effective stress; σ=total stress; u_a=pore air pressure; u_w=water pressure, the quantity $(u_a - u_w)$ is called matric suction; and χ is called the coefficient of effective stress and is a constitutive property of soil that depends on the degree of saturation. For saturated soil, the air pressure is zero, the water pressure is

[1]Professor, Colorado School of Mines, Division of Engineering, Golden, CO 80401. E-mail: ninglu@mines.edu

[2]Professor, Colorado School of Mines, Division of Engineering, Golden, CO 80401. E-mail: d.v.griffiths@mines.edu

Note. Discussion open until March 1, 2005. Separate discussions must be submitted for individual papers. To extend the closing date by one month, a written request must be filed with the ASCE Managing Editor. The manuscript for this paper was submitted for review and possible publication on March 29, 2002; approved on January 13, 2004. This paper is part of the ***Journal of Geotechnical and Geoenvironmental Engineering***, Vol. 130, No. 10, October 1, 2004. ©ASCE, ISSN 1090-0241/2004/10-1063–1076/$18.00.

compressive or positive, and χ is equal to one. Therefore the effective stress is the difference between total stress and pore water pressure. For a completely dry soil, χ is equal to zero, and the effective stress is the difference between total stress and air pressure. For partially saturated soil, χ is between zero and one, and reflects the proportion of matric suction $(u_a - u_w)$ that contributes to effective stress. The parameter χ will be referred to as the coefficient of effective stress hereafter.

Role of Coefficient of Effective Stress χ

Understanding the dependency of the coefficient of effective stress χ on the degree of saturation for various soils has been a challenging task from both experimental and theoretical perspectives. The theoretical investigations have mainly focused on geometric consideration of spherical sand particles due to capillary suction mechanisms (e.g., Fisher 1926; Blight 1961; Sparks 1961; Iwata and Tabuchi 1988; Cho and Santamarina 2001). These studies considered the geometry of the water lens between spherical particles and employed the Young–Laplace equation to connect water lens geometry and size (saturation) to the matric suction. So far, only pendulur states (discontinuous water film) has been quantitatively analyzed. For ideal uniform spherical particles with simple cubic or closest packing, the pendular state represents a degree of saturation of less than 25%. In general, when the degree of saturation of sand is low, the variation of the χ parameter has been observed by Escario and Juca (1989) to be concave upward with respect to the degree of saturation, as shown in Fig. 1(a). For higher degrees of saturation, no analytical relation between the χ parameter and the degree of saturation has been reported owning to the complex geometry of water film interactions among particles. Some experimental results, however, depicted the relationship between χ and degree of saturation in the high saturation range for various types of soils (e.g., Donald 1961; Blight 1961) as also shown in Fig. 1(a).

In principle as shown in Eq. (1), if the suction stress and matric suction could be measured independently, the coefficient of effective stress χ would follow. Although the matric suction can be measured with some confidence, it is not possible at the present time to directly measure the suction stress, thus no direct measurement of χ is available. An alternative way to obtain the χ parameter proposed by Bishop (1954) was based on the stresses occurring in a soil specimen at failure. In order to represent failure conditions in an unsaturated soil specimen, a Coloumb criterion was used

$$\tau_f = c' + \sigma' \tan \phi' \tag{2}$$

which, after substitution of the effective stress expression from Eq. (1), leads to

$$\tau_f = c' + [(\sigma - u_a)_f + \chi_f (u_a - u_w)_f] \tan \phi' \tag{3}$$

where τ_f=shear strength; c' and ϕ'=effective shear strength parameters; and the subscript f represents the parameter or stress variables at the state of failure.

In a typical direct shear test, the net total stress $(\rho - u_a)$ is known, and the net effective stress can be deduced from the shear stress at failure. Hence, by measuring the matric suction $(u_a - u_w)$, the coefficient of effective stress χ can be deduced. Since the matric suction at failure can define the degree of saturation by way of the soil water characteristics curve (SWCC), a one-to-one relationship between χ and the degree of saturation can be established. Fig. 1(a) also shows some previous experimental data from shear tests on soils with relatively high degrees of saturation (or low suction), where the coefficient of effective stress χ displays a concave downward nature with respect to the degree of saturation.

Possible Practical Forms for Coefficient of Effective Stress χ

Based on the failure experiments, Bishop proposed a slightly nonlinear form of χ, as shown in Fig. 1(b). Several other mathematical forms of χ have also been proposed for unsaturated soils. In some cases, the coefficient of effective stress χ is expressed as a function of the degree of saturation [e.g., Vanapalli et al. 1996; and Oberg and Sallfors 1997, as shown in Fig. 1(b)], and others considered the coefficient of effective stress χ as a function of effective stress (e.g., Khalili and Khabbaz 1998; Bao et al. 1998). Both these approaches are fundamentally the same, since the matric suction and degree of saturation are related through the SWCC.

The validity of several recently proposed forms of χ was examined by Vanapalli and Fredlund (2000), where a series of shear strength test results on clay, silt, and sand by Escario and Juca (1989) were used. For a suction range between 0 and 15,000 kPa, the following two forms showed a good fit to the experimental results:

$$\chi = \left(\frac{\theta_w}{\theta_s}\right)^{\kappa} = \left(\frac{V_w}{V_v}\right)^{\kappa} = S^{\kappa} \tag{4}$$

and

$$\chi = \frac{\theta_w - \theta_r}{\theta_s - \theta_r} = \frac{S - S_r}{1 - S_r} \tag{5}$$

where the right-hand side of Eq. (5) is called the effective degree of saturation; θ_w=volumetric water content; θ_s=saturated volumetric water content; θ_r=residual volumetric water content; κ=fitting parameter; V_w=volume of water; V_v=volume of voids; S=degree of saturation; and S_r=residual degree of saturation that appears in many SWCC models. The nature of Eqs. (4) and (5) is illustrated in Fig. 1(b). The residual degree of saturation can be defined conceptually as the degree of saturation at which any further increase in matric suction will not result in a significant change in the degree of saturation.

Comparing Figs. 1(a and b), it is evident that the power form [Eq. (4)] provides some flexibility to fit χ between the measured and predicted values. However, it does not predict the concave downward behavior in the high degree of saturation range. By incorporating the residual saturation (horizontal line for the degree of saturation less than S_r) Eq. (5) also can reflect concave upward behavior near the low degree of saturation. Since this equation does not involve the extra fitting parameter κ, it will be used in this study. With this form of the coefficient of effective stress χ in conjunction with Eq. (1), it will be possible to analyze unsaturated soil stress problems in a consistent effective stress framework, in which classical saturated soil analysis simply becomes a special case. The effective stress profiles in unsaturated soil will be obtained by application of Eq. (5), and the Coulomb criterion from Eq. (3) can then be used to assess the stability of unsaturated soils.

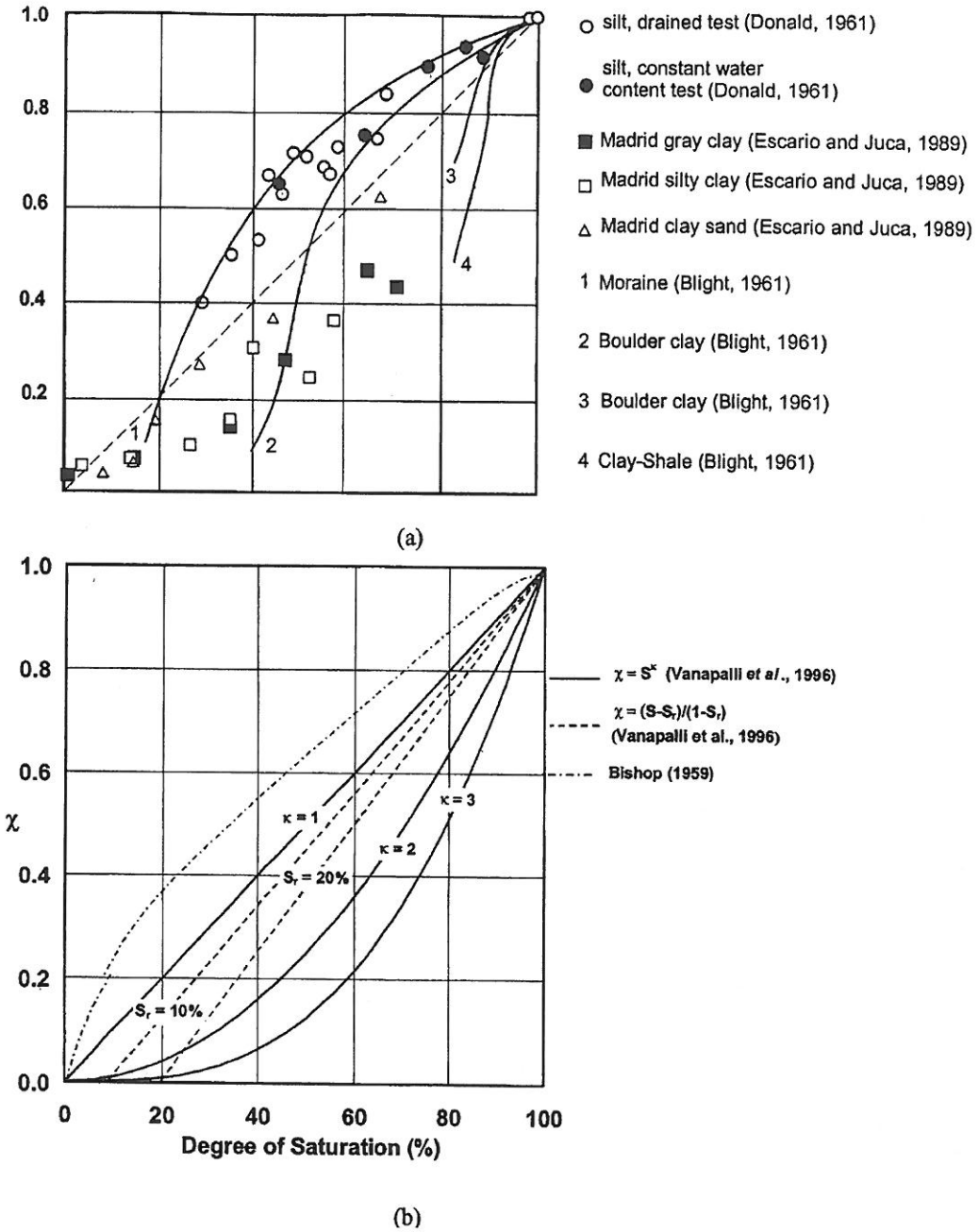

Fig. 1. Coefficient of effective stress: (a) some previous experimental and theoretical results, and (b) experimentally validated forms proposed by Vanapalli et al. (1996) and Vanapalli and Fredlund (2000)

Soil Water Characteristic Curve

The SWCC describes the relationship between matric suction and soil water content or the degree of saturation. The SWCC varies widely for different soil types as shown in Fig. 2 for three different soils: sand, silt, and clay, where α and n are pore size parameters (e.g., Gardner 1958; Van Genuchten 1980; Singh 1997). The physical interpretation of the SWCC lies in a soil's ability to sustain a particular degree of saturation under a given matric suction. For example, at a soil suction of 1,000 kPa, sand can only sustain a degree of saturation of a few percent, for silt this value increases to about 10%, whereas in clay, it increases further to several tens of percent. At higher matric suctions, the degree of saturation tends to a low constant value called the residual degree of saturation, S_r. At lower matric suctions, the curve is quite flat and insensitive to the degree of saturation. The point at which the degree of saturation starts to become sensitive to the matric suction is when air starts to enter pore space. The suction value corresponding to this transition point is often called the air entry pressure.

The air entry pressure and the residual saturation concepts have been used in many mathematical models of SWCC as benchmark values for different soils (e.g., Brooks and Corey 1964; Van Genuchten 1980; Fredlund and Xing 1994, among

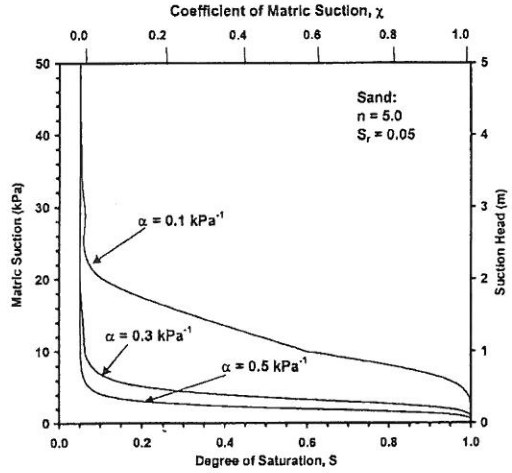

(a)

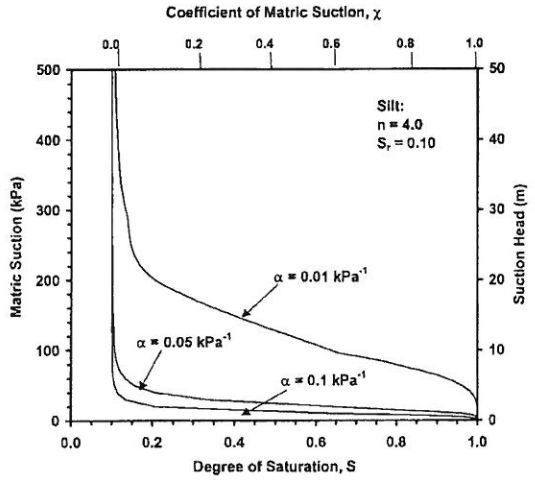

(b)

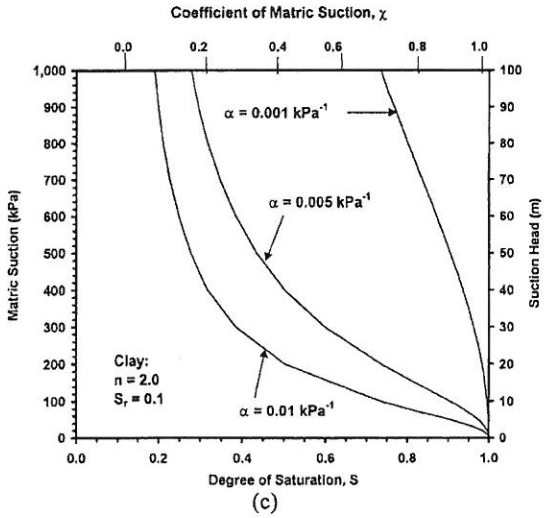

(c)

Fig. 2. Illustration of the representative solid water characteristics curve and χ functions for (a) sand, (b) silt, and (c) clay

Table 1. Range of Soil Parameters for Various Soils

Soil type	n (dimensionless)	α (kPa^{-1})	S_r (%)	k_s (m/s)
Sand	4–8.5	0.1–0.5	5–10	10^{-2}–10^{-5}
Silt	2–4	0.01–0.1	8–15	10^{-6}–10^{-9}
Clay	1.1–2.5	0.001–0.01	10–20	10^{-9}–10^{-13}

many others). The Van Genuchten's model is used in this study due to its ability to facilitate closed form analytical solutions for suction stress profiles, with a minimum number of parameters.

In the Van Genuchten's model, the effective degree of saturation is expressed as a function of matric suction

$$\frac{S-S_r}{1-S_r}=\left(\frac{1}{1+[\alpha(u_a-u_w)]^n}\right)^{1-1/n} \tag{6}$$

where α and n=pore size parameters. The parameter n has been shown (e.g., Van Genuchten 1980; Singh 1997) to lie in the range $1.1<n<8.5$. The parameter α is the inverse of the air entry pressure and lies in the range $0<\alpha<0.5$ kPa^{-1}. Typical values of the unsaturated soil parameters are given in Table 1. For reference, the range of typical values of the saturated hydraulic conductivity k_s is also listed in Table 1.

Substituting Eq. (6) into Eq. (5) yields

$$\chi=\left(\frac{1}{1+[\alpha(u_a-u_w)]^n}\right)^{1-1/n} \tag{7}$$

Values of the coefficient of effective stress χ for different soil types have been included on the top horizontal axis of the SWCC curves in Fig. 2.

Vertical Profiles of Matric Suction

The vertical distribution of matric suction in a horizontally layered unsaturated soil generally depends on several factors: in particular, the soil properties as given by the SWCC and the soil permeability characteristic curve (SPCC), environmental factors including infiltration due to precipitation or evaporation rates, and boundary drainage conditions including the location of the water table. The combination of these factors results in different matric suction profiles as shown in Fig. 3.

The vertical profile of matric suction, and how it is influenced by infiltration or evaporation, has been an important area of study

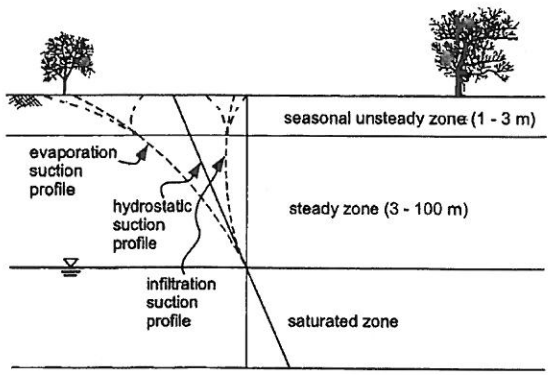

Fig. 3. Conceptual model of suction in horizontally layered unsaturated soil profiles under various surface flux boundary conditions

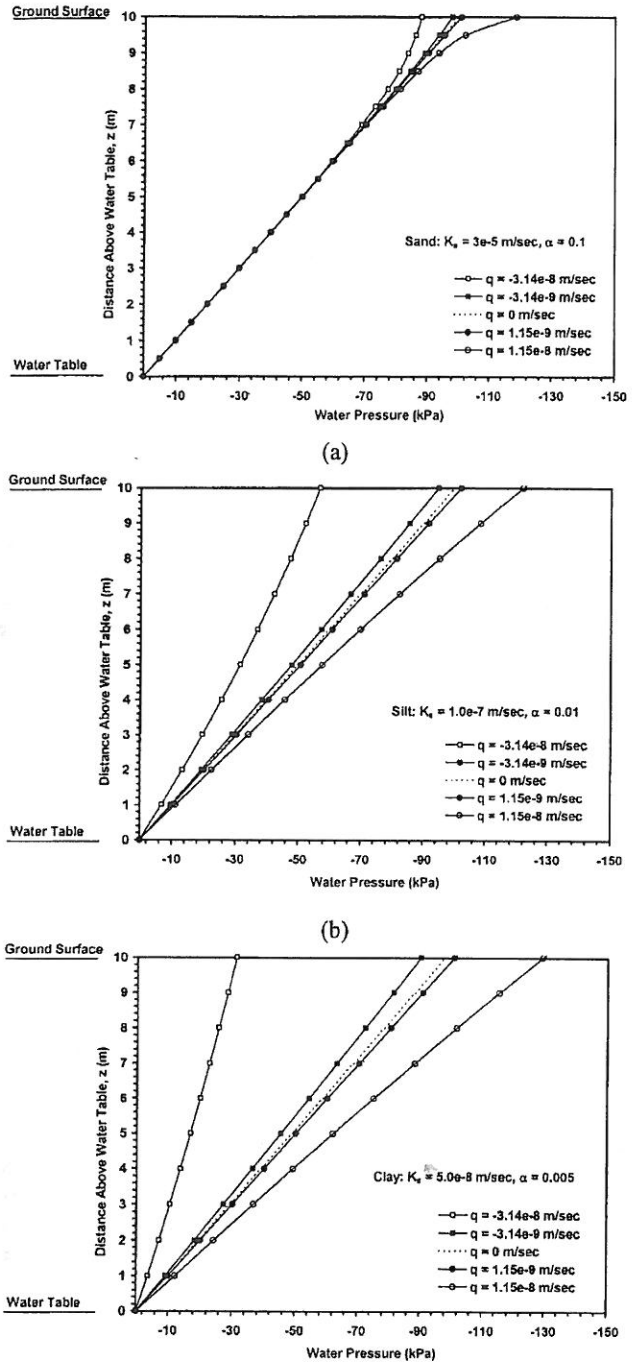

Fig. 4. Suction profiles and the coefficient of effective stress profiles in various representative soils: (a) sand, (b) silt, and (c) clay

for many researchers (e.g., Bear 1975; Yeh 1989; Wilson 1997). Although matric suction profile within the seasonal unsteady state zone could be important to the stability of many shallow geotechnical structures (e.g., Rahardjo and Leong 1997; Totoev and Kleeman 1998; Fredlund et al. 2001), the present work focuses on developing the matric suction and suction stress profiles within the steady zone (Fig. 3). Such an approach is theoretically desirable and practically attractive since it is consistent with many

Table 2. Range of Infiltration (−) and Evaporation (+) Rates

Flux (m/s)	Flux (mm/d)	Flux (m/y)
-3.14×10^{-8}	−2.73	−1.000
-3.14×10^{-9}	−0.273	−0.100
0 (hydrostatic)	0	0
1.15×10^{-9}	0.1	0.0365
1.15×10^{-8}	1.0	0.365

classical earth pressure analyses such as horizontal stress profile at rest, Rankine's active and passive lateral earth pressure profiles, etc. Thus the theoretical framework presented in this paper is ready for direct application to expand the classical limit analysis to unsaturated soil environments. The mathematical prediction of matric suction profiles can be established by solving the governing flow equation with appropriate initial and boundary conditions. For steady-state profiles, Darcy's law can describe the vertical unsaturated flow rate as

$$q=-k\left(\frac{d(u_a-u_w)}{\gamma_w dz}+1\right) \tag{8}$$

where k=unsaturated hydraulic conductivity dependent on matric suction; and γ_w=unit weight of water.

To describe the characteristic of unsaturated hydraulic conductivity, Gardner's model (1958) is used

$$k=k_s e^{-\alpha(u_a-u_w)} \tag{9}$$

where k_s=saturated hydraulic conductivity (m/s); and α=inverse of the air entry pressure (kPa^{-1}) as defined previously. Gardner's permeability model has been widely used to obtain many analytical solutions of unsaturated flow problems (e.g., Phillips 1987).

With Eqs. (8) and (9), and the boundary condition of zero suction at the water table ($z=0$) and a steady-state flow rate q (negative for downward infiltration and positive for upward evaporation), we can arrive at an analytical solution for the suction head as follows (see derivation in Appendix I):

$$(u_a-u_w)=\frac{-1}{\alpha}\ln[(1+q/k_s)e^{-\alpha\gamma_w z}-q/k_s] \tag{10a}$$

The above equation can be rewritten in terms of dimensionless matric suction $\alpha(u_a-u_w)$, depth $\gamma_w\alpha z$, and flow ratio q/k_s as

$$\alpha(u_a-u_w)=-\ln[(1+q/k_s)e^{-\alpha\gamma_w z}-q/k_s] \tag{10b}$$

Profiles of matric suction for various soils and flow ratio are illustrated in Fig. 4. The typical parameters for different soils are listed in Table 1, and a range of common infiltration and evaporation rates are listed in Table 2. It is shown in Fig. 4(a), for example, that in a sandy soil, different steady flow rates only start to have an influence on the matric suction at heights of about 8 m or more above the water table. The matric suction at 10 m above the water varies by about 20 kPa, ranging from maximum matric suction for evaporation to minimum matric suction for infiltration.

For a typical silty soil behavior as shown in Fig. 4(b), the steady flow rate has a greater influence on the matric suction profile. In this case, the matric suction change zone reaches the water table and the maximum change occurs at the highest infiltration rate. The trend continues for even finer grained soils such as clay, as shown in Fig. 4(c). In this case, the maximum matric suction change can reach about 60 kPa under the highest infiltration rate. The high changes in the matric suction profile in fine-

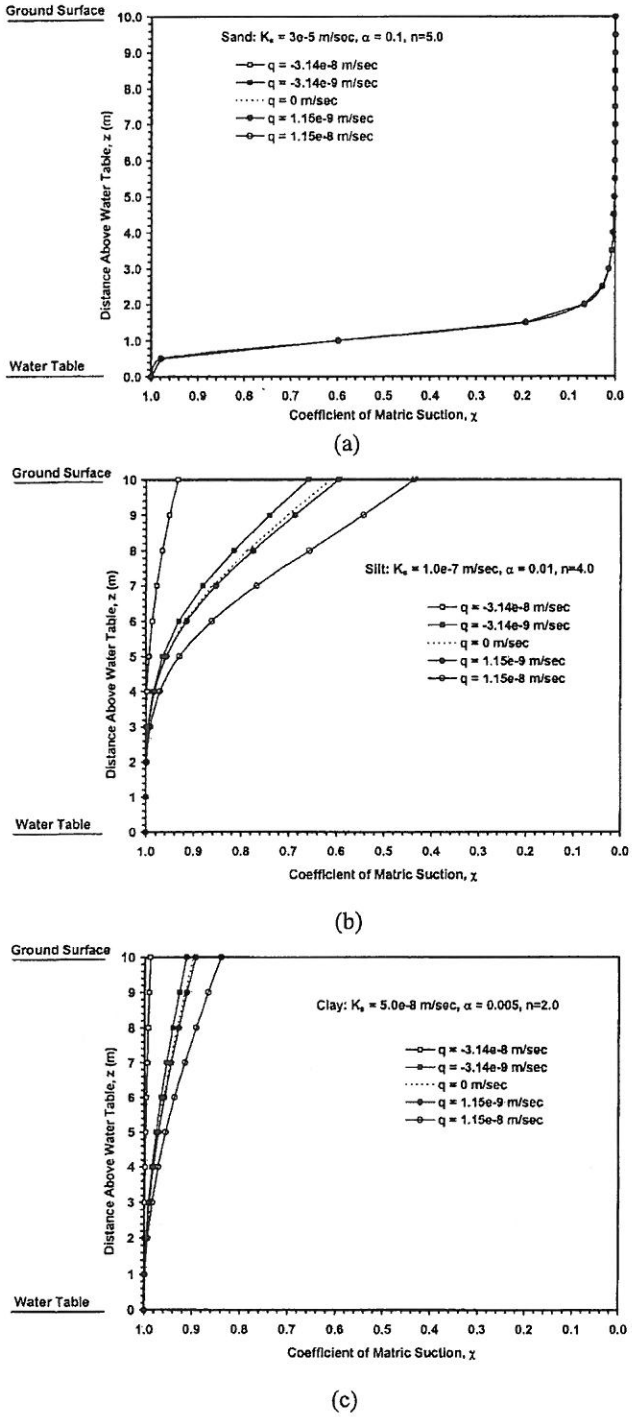

Fig. 5. Coefficient of effective stress profiles under various surface flux boundary conditions in various representative soils: (a) sand, (b) silt, and (c) clay

grained soils predicted by this model are consistent with physical reasoning and previous field and laboratory observations.

It may be noted that in all cases shown in Fig. 4, the matric suction distribution corresponding to zero infiltration is predicted by Eq. (10*a*) to be a simple linear extrapolation of the hydrostatic pressure.

Profiles of Effective Stress Coefficient χ

The vertical profile of the coefficient of effective stress as a function of the dimensionless depth $\gamma_w \alpha z$ and flow ratio q/k_s can be derived by substituting Eq. (10*b*) into Eq. (7)

$$\chi = \left(\frac{1}{1 + \{- \ln[(1 + q/k_s)e^{-\gamma_w \alpha z} - q/k_s]\}^n} \right)^{1-1/n} \tag{11}$$

The patterns of the vertical profiles for various values of the dimensionless depth $\gamma_w \alpha z$ and flow ratio q/k_s are illustrated in Fig. 5. It is clear from Fig. 5(a) that the coefficient of effective stress for sandy soil is insensitive to flow rates and falls quite rapidly above the water table, reaching zero at a height of about 4 m. The reduction in the coefficient of effective stress in silt and clay is much less pronounced, as shown in Figs. 5(b and c). Clay has the smallest variation in the coefficient of effective stress, with a less than 20% reduction within 10 m of the water table. In all cases, the coefficient of effective stress reduces with height above the water table, however, the reduction is greatest with evaporation and least with infiltration.

Profiles of Suction Stress and Its Solution Regimes

The suction stress that directly contributes to the effective stress in a soil as described in Eq. (1) can be obtained by combining Eqs. (10*b*) and (11) as follows:

$$\chi(u_a - u_w) = \frac{-1}{\alpha} \frac{\ln[(1 + q/k_s)e^{-\gamma_w \alpha z} - q/k_s]}{(1 + \{- \ln[(1 + q/k_s)e^{-\gamma_w \alpha z} - q/k_s]\}^n)^{(n-1)/n}} \tag{12}$$

or in a dimensionless form

$$\chi(u_a - u_w)\alpha = \frac{- \ln[(1 + q/k_s)e^{-\gamma_w \alpha z} - q/k_s]}{(1 + \{- \ln[(1 + q/k_s)e^{-\gamma_w \alpha z} - q/k_s]\}^n)^{(n-1)/n}} \tag{13}$$

Eq. (13) provides a general analytical way to calculate steady vertical suction stress profiles in unsaturated soils. There are only three soil parameters involved; α, n, and k_s. These three parameters define the SWCC and SPCC. The dimensionless *flow ratio* varies in the range $-1 < q/k_s$. Although Eq. (13) is a smooth and continuous function, it has some distinct characteristics in terms of its shape, maxima, and asymptotes. These characteristics are analyzed in detail in Appendix II, however, the solution of Eq. (13) can be conveniently subdivided into four solution regimes as shown in Fig. 6. A description of the properties and physical implications of each regime are summarized in the following sections.

Regime I: $0 \leq q/k_s$ and $n > 2.0$

This is the steady evaporation case. Profiles of suction stress exhibit a constant maximum value for all normalized flow rates q/k_s that depends only on the parameter n as follows:

$$[\chi(u_a - u_w)\alpha]_{\max} = \frac{(n-2)^{(n-2)/n}}{(n-1)^{(n-1)/n}} \tag{14}$$

The maximum suction stress occurs at the following depth:

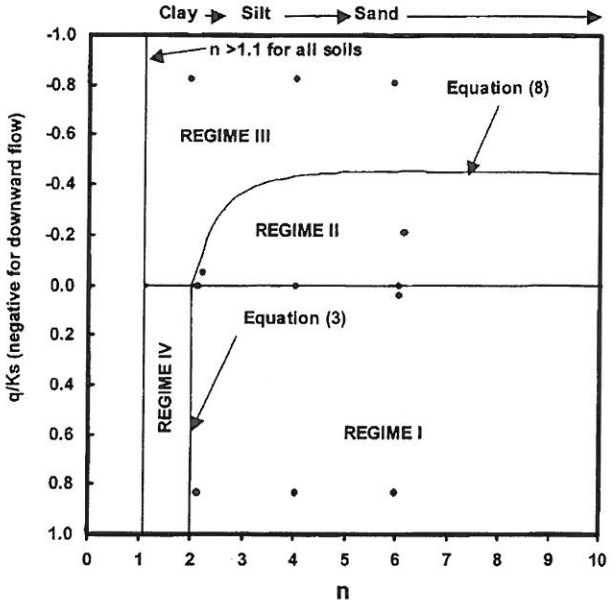

Fig. 6. Characteristic regimes of suction stress profiles; Regime I: maximum suction stress with zero asymptotic postmaximum suction stress, Regime II: maximum suction stress with a finite asymptotic postmaximum suction stress, Regime III: monotonic increasing suction stress, and Regime IV: maximum suction stress with a rapidly decreasing asymptotic postmaximum suction stress of zero

$$(\alpha\gamma_w z)_{\max} = \ln\left\{\frac{(1+q/k_s)e^{(n-2)^{-1/n}}}{1+\frac{q}{k_s}e^{(n-2)^{-1/n}}}\right\} \tag{15}$$

After passing the maximum value, the suction stress decreases and tends to zero as the normalized depth $\alpha\gamma_w z$ approaches to $\ln(1+k_s/q)$. For $\alpha\gamma_w z > \ln(1+k_s/q)$, the solution to Eq. (10*a*) is undefined (see Appendix I). The normalized suction profiles for various normalized flow ratios are illustrated in Fig. 7(a).

A limiting case is the so-called "hydrostatic" case, when $q/k_s=0$. The suction stress profile has a maximum value expressed by Eq. (14), and the location of the maximum suction stress can be obtained by imposing the zero value of the flow ratio on Eq. (15), hence

$$(\alpha\gamma_w z)_{\max} = (n-2)^{-1/n} \tag{16}$$

After passing the maxium value, the suction stress decreases and tends to zero as the normalized depth $\alpha\gamma_w z$ tends to infinity (see Appendix II). The normalized suction profiles in the "hydrostatic" case for various values of the soil parameter n are illustrated in Fig. 7(b).

Regime II: $-e^{-(n-2)^{-1/n}} < q/k_s < 0$

This is the "small" steady infiltration case. The suction stress reaches the same maximum at the same depth as it did in Regime I

$$(\alpha\chi u_w)_{\max} = \frac{(n-2)^{(n-2)/n}}{(n-1)^{(n-1)/n}} \tag{17}$$

and the maximum suction stress occurs at the following distance above the water table:

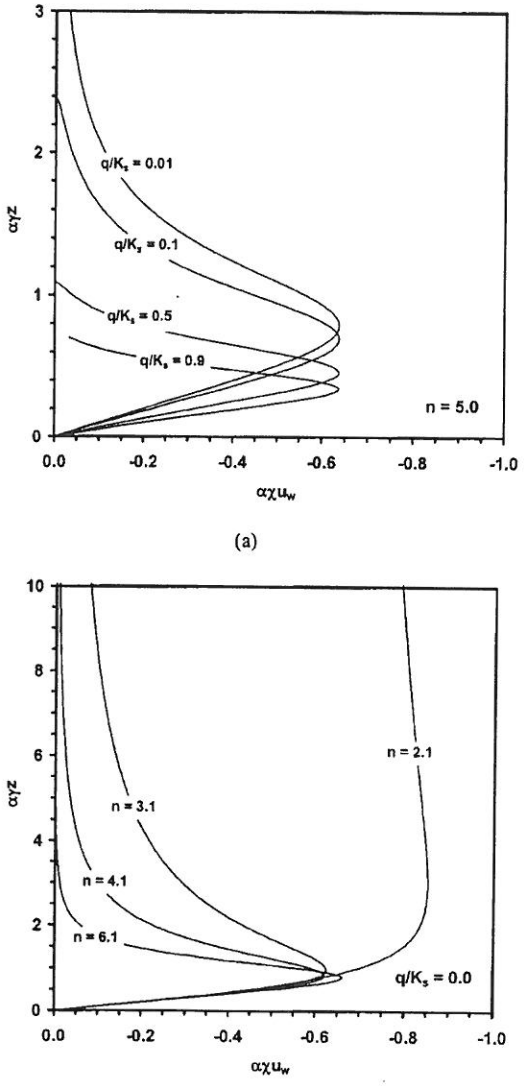

Fig. 7. Suction stress profiles in Regime I: (a) for various evaporation rates, and (b) for various soil parameter n

$$(\alpha\gamma_w z)_{\max} = \ln\left\{\frac{(1+q/k_s)e^{(n-2)^{-1/n}}}{1+\frac{q}{k_s}e^{(n-2)^{-1/n}}}\right\} \tag{18}$$

An interesting and unique behavior of this regime is that, after passing the maximum value, the suction stress decreases and asymptotically approaches the following value that is dependent on both the soil parameter n and the flow ratio q/k_s:

$$[\alpha\chi(u_a-u_w)]_{\alpha\gamma_w z\to\infty} = \frac{-\ln\left(-\frac{q}{k_s}\right)}{\left\{1+\left[-\ln\left(-\frac{q}{k_s}\right)\right]^n\right\}^{(n-1)/n}} \tag{19}$$

The normalized suction profiles for various infiltration ratio q/k_s are illustrated in Fig. 8(a). The normalized suction profiles for various n values are shown in Fig. 8(b)

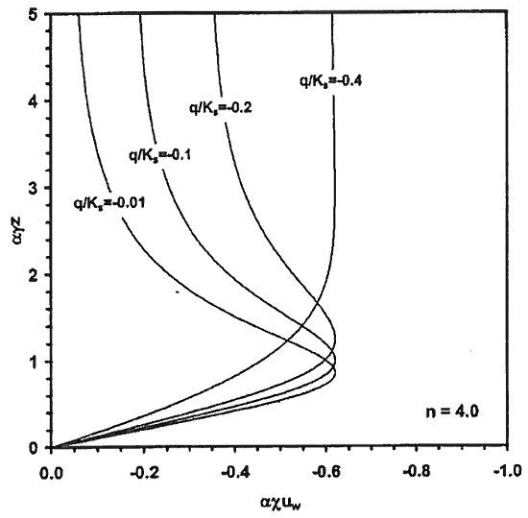

(a)

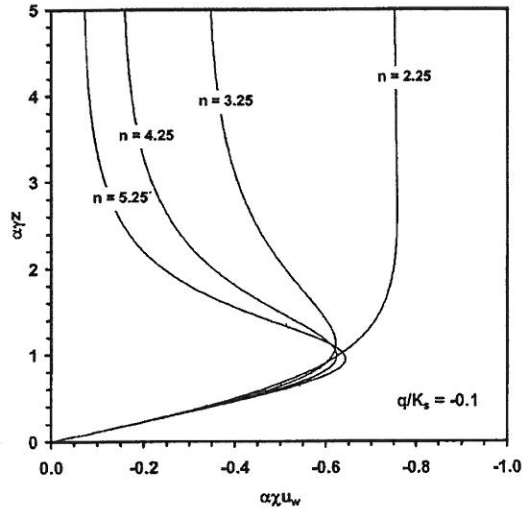

(b)

Fig. 8. Suction stress profiles in Regime II: (a) for various infiltration rates, and (b) for various soil parameter n

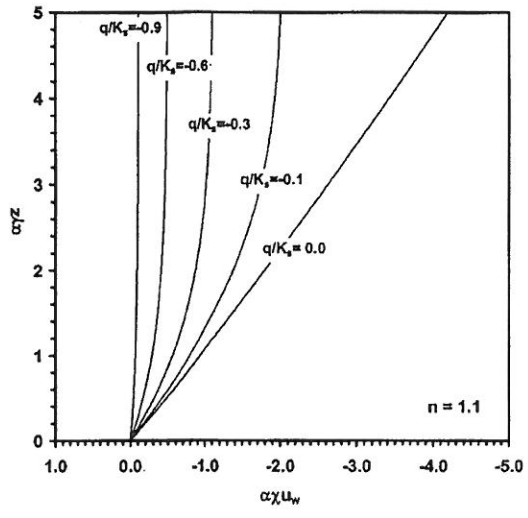

(a)

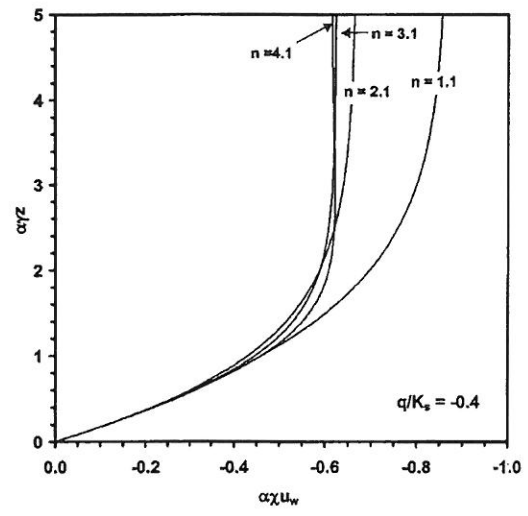

(b)

Fig. 9. Suction stress profiles in Regime III: (a) for various infiltration rates, and (b) for various soil parameter n

Regime III: $-1<q/k_s\leq -e^{-(n-2)^{-1/n}}$, $n\geq 2$; $q/k_s<0$, $1.1<n<2$

This is the "large" steady infiltration case. The suction stress increases as the distance above the water table increases, and approaches asymptotically to the following value:

$$[\alpha\chi(u_a-u_w)]_{\alpha\gamma_w z\to\infty}=\frac{-\ln\left(-\dfrac{q}{k_s}\right)}{\left\{1+\left[-\ln\left(-\dfrac{q}{k_s}\right)\right]^n\right\}^{(n-1)/n}} \tag{20}$$

which is equal to the asymptotic value of postmaximum suction stress in Regime II [Eq. (19)]. The normalized suction profiles for various values of infiltration ratio q/k_s are illustrated in Fig. 9(a) for the case of $n=1.1$.

A limiting case is $q/k_s=-e^{-(n-2)^{1/n}}$ where suction stress profiles become varying monotonically with the distance from the water table. The suction stress increases as the distance from the water table increases and approaches asymptotically to the following value:

$$[\alpha\chi(u_a-u_w)]_{\alpha\gamma_w z\to\infty}=\frac{(n-2)^{(n-2)/n}}{(n-1)^{(n-1)/n}} \tag{21}$$

which is equal to the maximum suction stress value in Regime II [Eq. (17)]. Under this limiting case, the maximum suction stress is no longer a function of the normalized flow ratio, but is solely a function of the soil parameter n. The normalized suction profiles for various soil parameter n values are illustrated in Fig. 9(b). A smooth transition between Regimes II and III is also illustrated in Fig. 9(b) for the flow ratio of -0.434, where $n=4.1$ is in Regime II with a maximum matric suction $\alpha\chi(u_a-u_w)=0.622$ at $\alpha\gamma_w z$

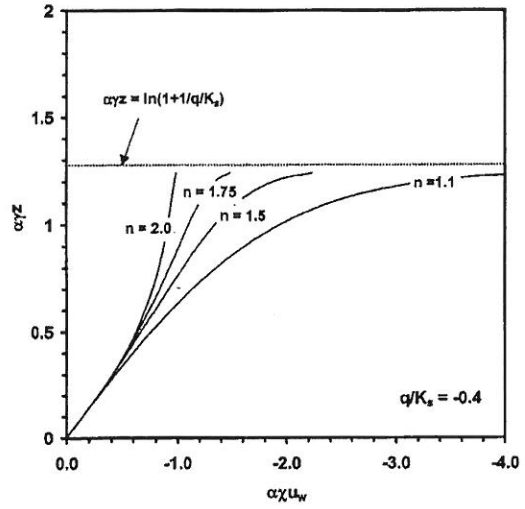

(a)

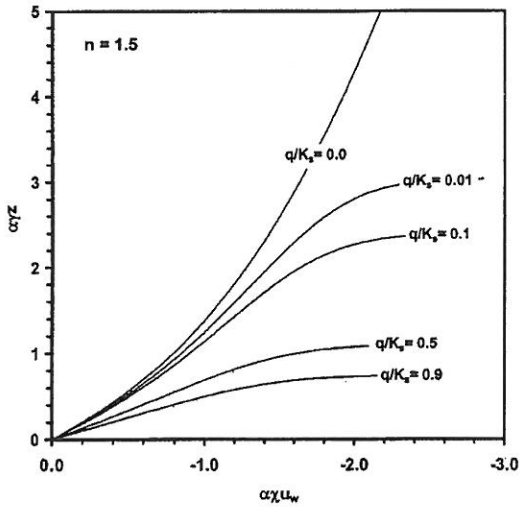

(b)

Fig. 10. Suction stress profiles in Regime IV: (a) for various soil parameter n, and (b) for various infiltration rates

$=2.2$. In Fig. 9(a), $q/k_s=0$ is also plotted to illustrate the transition from Regime III to Regime IV.

Regime IV: $0 \leq q/k_s$ and $1.1 < n \leq 2.0$

This is the "dry clayey soil" evaporation case. The maximum suction stress [Eq. (14)] always occurs at $\alpha\gamma_w z = \ln(1+k_s/q)$ [Fig. 10(a)]. After passing the maximum suction stress point, the suction stress quickly approaches to infinity as $\alpha\gamma_w z \rightarrow \ln(1+k_s/q)$. For $n=2$, the dimensionless suction stress tends to 1 as $\alpha\gamma_w z \rightarrow \ln(1+k_s/q)$. For $\alpha\gamma_w z \geq \ln(1+k_s/q)$, the solution of the suction stress is undefined (Appendixes I and II). Another feature of the suction stress profile in this regime is that it is very sensitive to the evaporation rate as shown in Fig. 10(b). This feature is due to the high dependency of the suction profile on the evaporation rate [Eq. (10*b*)], and this feature has been pointed out in previous works (e.g., Bear 1975; Marshall and Holmes 1988; Stephens 1995).

Assessment of Profiles of Suction Stress in Representative Unsaturated Soils

Application of the analytical solution given by Eq. (13) to representative soils of sand, silt, and clay is presented here to illustrate the magnitude and general patterns of the suction stress profiles in unsaturated soils. Typical ranges of steady infiltration and evaporation are listed in Table 2. Representative soil parameters are listed in Table 1. Soil saturation and suction stress profiles under the hydrostatic condition of zero flow rate are first examined. The hydrostatic suction stress profiles follow the characteristics of Regimes I and II for sand and silt but follow the characteristics of Regime III for clay as described in the previous section. The suction profile, despite types of soil, follows the linear distribution predicted by Eq. (10*a*). Soil saturation profiles can then be calculated by using Eq. (6) (Fig. 2) and the suction stress profiles by employing Eq. (13) (Fig. 11) for various soil parameters.

It can be seen (Fig. 11) that the α parameter strongly controls the shape of the soil saturation profiles and the magnitude and shape of the suction stress profiles. Large α values represent large pore sizes, thus a short influence distance of water retention above the water table and hence small suction stresses.

It can also be observed [Fig. 2(a)] that in unsaturated sand, water retention becomes insignificant at a distance of about 2 m above the water table. The maximum suction stress could reach 6.4 kPa at about 1.2 m above the water table [Fig. 12(a)]. In an unsaturated silt layer [Fig. 2(b)], the significant distance for water retention extends to about 20 m, and the maximum suction stress could reach 64 kPa at 9 m above the water table. Evaporation causes a downward shift of the location of the maximum suction stress. In an unsaturated clay layer, the significant distance for water retention could be greater than 100 m [Fig. 2(c)], and the maximum suction stress could reach 700 kPa. Under the steady infiltration condition most clay soils follow the characteristics of Regime III ($1.0 < n < 2.0$), and the suction stress increases nearly linearly as the distance is away from the water table [Fig. 12(c)]. Under the steady evaporation condition most clay soils follow the characteristics of Regime IV. Since clay soils have very small values of α typically between 0.01 and 0.001 kPa^{-1}, the value of $\alpha\gamma_w z$ is very small for a soil layer less than 10 m thick. The small value of $\alpha\gamma_w z$ leads to the suction stress varying nearly linearly in the vertical direction as shown in Fig. 12(c).

The fact that a maximum suction stress can occur within an unsaturated soil layer of sand or silt implies that the effective stress could also reach a maximum. It can also be concluded (see Fig. 12) that in an unsaturated soil layer 10 m thick, for example, the maximum suction stress could reach 110 kPa in clay, 60 kPa in silt, and 6 kPa in sand. This magnitude of suction stress ranging from 6 to 110 kPa can be important in many foundation analyses, such as retaining wall design, bearing capacity, and slope stability.

It can also be concluded that for an unsaturated sand layer 10 m thick, suction stresses will modify the effective stress profile mostly near the water table, whereas in finer grained soils such as silt or clay, the suctions can have a significant influence on the effective stresses throughout the entire layer. Under the steady state flow rates, including both downward infiltration and upward evaporation, all four characteristic regimes can occur in real soils.

Summary and Conclusions

Rigorous application of the effective stress principle to unsaturated geotechnical engineering problems requires an explicit

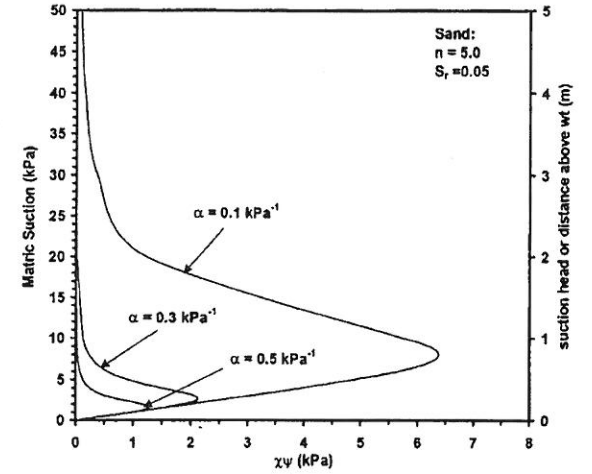

(a)

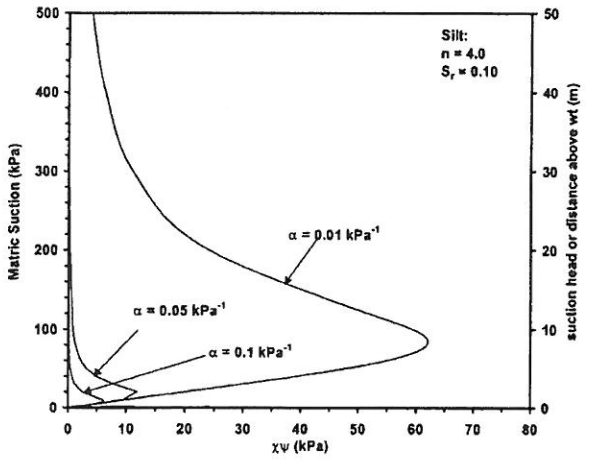

(b)

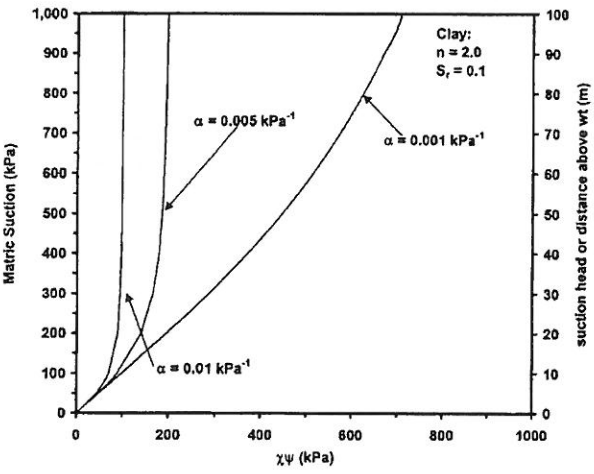

(c)

Fig. 11. Suction stress profiles in representative soils under hydrostatic condition: (a) sand, (b) silt, and (c) clay

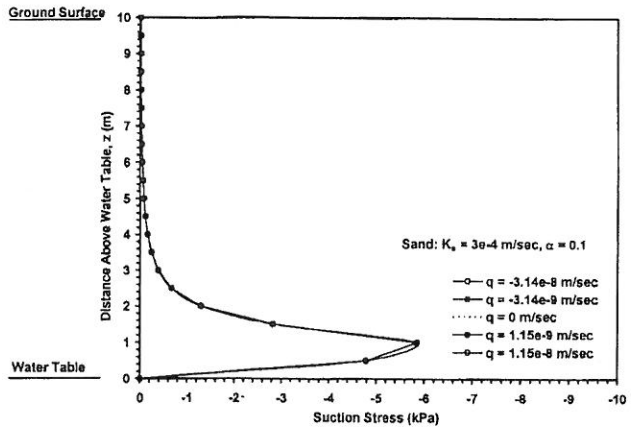

(a)

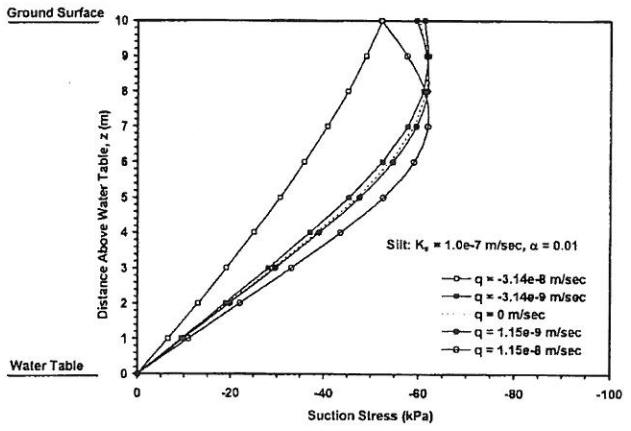

(b)

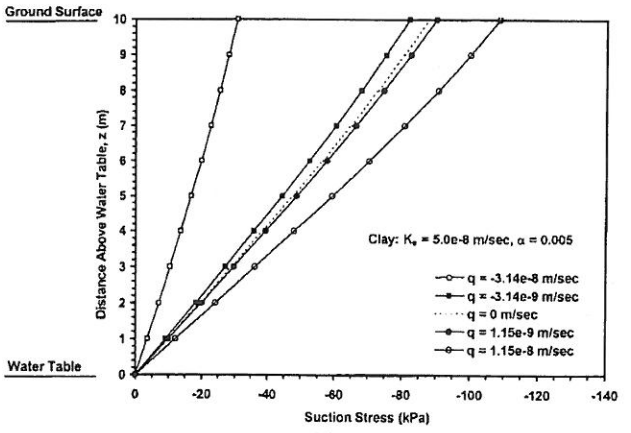

(c)

Fig. 12. Suction stress profiles in representative soils under different surface flux boundary conditions: (a) sand, (b) silt, and (c) clay

knowledge of the contribution to effective stress due to tensile pore water pressures above the water table. This stress has been referred to throughout this paper as the suction stress. The suction stress depends on the matric suction $(u_a - u_w)$ and the matric suction coefficient χ.

The matric suction coefficient is expressed in terms of the equivalent degree of saturation, based on some recent experimental verification. The commonly available unsaturated soil charac-

teristic curves, namely the SWCC and SPCC, are formally adapted to produce a closed form expression for the suction stress profile for different soil types and steady state flow rate conditions. The SWCC is used to better represent the coefficient of effective stress, and the SPCC is used to arrive at a general suction profile. The general characteristics of the suction stress profile are highly dependent on soil type and steady flow rate, and are illustrated in four distinct regimes using the dimensionless distance and suction stress.

The likely patterns and magnitude of the profiles of matric suction and suction stress in typical soils of sand, silt, and clay are analyzed under several possible flow rate ranges of infiltration and evaporation. In a sandy layer 10 m thick, the impact of steady infiltration and evaporation is limited to near the ground surface. The maximum matric suction decrease, compared to the hydrostatic condition, is about 20 kPa for a steady evaporation rate of 1 mm/day, and about 10 kPa for a steady infiltration of 2.73 mm/day. The corresponding changes in the suction stress are hardly seen in the suction stress profile. The maximum suction stress occurs at about 1.2 m above the water table and is about 6 kPa.

In a silty layer, the maximum matric suction decrease due to the 1 mm/day evaporation rate is about 20 kPa, about the same in the sandy layer. However, the changes in the matric suction profile extend throughout the entire layer thickness. The maximum matric suction increase due to the infiltration rate of 2.73 mm/day reaches about 40 kPa, compared to the hydrostatic condition, and extends over the entire layer thickness. The corresponding suction stress profiles give a maximum suction stress of about 60 kPa, with the maximum occurring 6–8 m above the water table.

In a clayey layer 10 m thick, the matric suction profiles are greatly affected by the steady flow rate, with a maximum suction change exceeding 65 kPa for an infiltration rate of 2.73 mm/day. The suction stress profiles vary nearly linearly in the vertical direction, with the maximum suction stress change of 60 kPa for an infiltration rate of 2.73 mm/day.

In conclusion, the theory provides a general quantitative way to calculate vertical suction stress profiles in various unsaturated soils under steady flow rate conditions, once the soil's SWCC and SPCC are known. The theory is consistent in the form of stress profile with the classical limit analysis such as Rankine's active and passive lateral earth pressure profiles. The theory retains the simplicity and generality of the principle of effective stress, and thus in conjunction with other analysis tools, can be directly applied to the study of classical geotechnical problems such as earth pressures, slope stability, bearing capacity, and waste containment systems.

Appendix I. Derivation of Steady-State Matric Suction Profile

Under the coordinate system of upward positive, the vertical specific discharge q (in m/s) can be described by Darcy's law as

$$q = -k\left(\frac{d\psi}{dz} + 1\right) \tag{22}$$

where k=hydraulic conductivity depending on suction head Ψ [$\Psi = -(u_a - u_w)/\gamma_w$, in m].

To describe the characteristic of unsaturated hydraulic conductivity, Gardner's model (1958) is used

$$k = k_s e^{(\beta\psi)} \tag{23}$$

where k_s=saturated hydraulic conductivity in m/s, and β=pore size distribution parameter equal to $\gamma_w\alpha$ describing the rate of reduction in hydraulic conductivity.

With Eqs. (22) and (23), and the boundary condition of zero suction at the water table ($z=0$), we can arrive at an analytical solution for the suction profile as follows.

Substituting Eq. (23) into Eq. (22) leads to

$$q = -k_s e^{\beta\psi}\left(\frac{d\psi}{dz} + 1\right)$$

$$-\frac{q}{k_s}dz = e^{\beta\psi}d\psi + e^{\beta\psi}dz \tag{24}$$

$$dz = -\frac{e^{\beta\psi}d\psi}{e^{\beta\psi} + q/k_s} = -\frac{1}{\beta}\frac{d(e^{\beta\psi} + q/k_s)}{e^{\beta\psi} + q/k_s}$$

Integrating the above equation and imposing the zero suction at the water table $z=0$ leads to

$$\int_0^z dz = -\frac{1}{\beta}\int_0^{\psi}\frac{d(e^{\beta\psi} + q/k_s)}{(e^{\beta\psi} + q/k_s)}$$

$$-\beta z = \ln\frac{e^{\beta\psi} + q/k_s}{1 + q/k_s} \tag{25}$$

$$\psi = \frac{1}{\beta}\ln[(1 + q/k_s)e^{-\beta z} - q/k_s]$$

or in terms of matric suction $(u_a - u_w)$ and the parameter α

$$(u_a - u_w) = \frac{-1}{\alpha}\ln[(1 + q/k_s)e^{-\gamma_w\alpha z} - q/k_s] \tag{26}$$

By mathematical definition, the quantity in the bracket of the logarithm should be greater than zero. By physical constrain, the quantity in the bracket of the logarithm should be less than or equal to 1.0 to ensure the suction is negative or zero, i.e.

$$0 < (1 + q/k_s)e^{-\gamma_w\alpha z} - q/k_s \leqslant 1.0$$

The requirement of less than or equal to 1.0 leads to the constraint that the downward infiltration flux q should be less than or equal to the saturated hydraulic conductivity, reasoned as follows:

$$(1 + q/k_s)e^{-\gamma_w\alpha z} - q/k_s \leqslant 1.0$$

$$q/k_s \geqslant \frac{1 - e^{-\gamma_w\alpha z}}{e^{-\gamma_w\alpha z} - 1} = -1 \tag{27}$$

$$q \leqslant k_s$$

Now let us go back to the constraint that the quantity in the bracket of the logarithm in Eq. (26) should be greater than zero, i.e.

$$0 < (1 + q/k_s)e^{-\gamma_w\alpha z} - q/k_s$$

When $1.0 \geqslant q/k_s > 0$ the above condition leads to

$$\gamma_w\alpha z < \ln\left(1 + \frac{k_s}{q}\right) \tag{28}$$

For the analytical solution (26) to be valid, the above inequality has to be satisfied. When the above condition is not satisfied, the

permissible solution for Eq. (25) or Eq. (24) is a trivial one

$$(u_a - u_w) = 0 \tag{29}$$

For the hydrostatic condition of $q=0$, Eq. (25) becomes the linear suction distribution:

$$(u_a - u_w) = z\gamma_w \tag{30}$$

Appendix II. Delineation of Suction Stress Regimes

From Eqs. (5) and (6), the suction stress coefficient χ is

$$\chi = \frac{1}{\{1 + [\alpha(u_a - u_w)]^n\}^{(n-1)/n}}$$

and from Appendix I, the matric suction $(u_a - u_w)$ is

$$u_a - u_w = \frac{-1}{\alpha}\ln\left[\left(1 + \frac{q}{k_s}\right)e^{-\gamma_w \alpha z} - \frac{q}{k_s}\right]$$

From Eq. (1), the suction stress is

$$\chi(u_a - u_w) = \frac{-1}{\alpha}\frac{-\ln\left[\left(1 + \frac{q}{k_s}\right)e^{-\gamma_w \alpha z} - \frac{q}{k_s}\right]}{\{1 + [-\alpha(u_a - u_w)]^n\}^{(n-1)/n}} \tag{31}$$

or in a dimensionless form

$$f(z) = \alpha\chi(u_a - u_w) = \frac{-\ln\left[\left(1 + \frac{q}{k_s}\right)e^{-\gamma_w \alpha z} - \frac{q}{k_s}\right]}{\{1 + [-\alpha(u_a - u_w)]^n\}^{(n-1)/n}} \tag{32}$$

The maxima can be found by setting $f'(z)=0$, i.e.

$$f'(z) = [\alpha\chi(u_a - u_w)]'$$

$$= 0 = \frac{[\alpha(u_a - u_w)]'\{1 + [\alpha(u_a - u_w)]^n\}^{(n-1)/n} - \ln\left[\left(1 + \frac{q}{k_s}\right)e^{-\gamma_w \alpha z} - \frac{q}{k_s}\right]\left(\frac{n-1}{n}\right)\{1 + [\alpha(u_a - u_w)]^n\}^{-1/n}(\alpha n)[\alpha(u_a - u_w)]^{n-1}(u_a - u_w)'}{\{1 + [\alpha(u_a - u_w)]^n\}^{(2n-2)/n}}$$

$$\{1 + [\alpha(u_a - u_w)]^n\}^{(n-1)/n} = \ln[(1 + q/k_s)e^{-\gamma_w \alpha z} - q/k_s](n-1)\{1 + [\alpha(u_a - u_w)]^n\}^{-1/n}[\alpha(u_a - u_w)]^{n-1}$$

$$[1 + [\alpha(u_a - u_w)]^n] = \ln[(1 + q/k_s)e^{-\gamma_w \alpha z} - q/k_s](n-1)[\alpha(u_a - u_w)]^{n-1}$$

$$\frac{[1 + [\alpha(u_a - u_w)]^n]}{(n-1)[\alpha(u_a - u_w)]^{n-1}} = \ln[(1 + q/k_s)e^{-\gamma_w \alpha z} - q/k_s]$$

$$\frac{[1 + [\alpha(u_a - u_w)]^n]}{(n-1)n[(1 + q/k_s)e^{-\gamma_w \alpha z} - q/k_s]^{n-1}} = \ln[(1 + q/k_s)e^{-\gamma_w \alpha z} - q/k_s] \tag{33}$$

$$\frac{\{1 + [\alpha(u_a - u_w)]^n\}}{(1-n)\{-\ln[(1 + q/k_s)e^{-\gamma_w \alpha z} - q/k_s]\}^{n-1}} = \ln[(1 + q/k_s)e^{-\gamma_w \alpha z} - q/k_s]$$

$$\{1 + [\alpha(u_a - u_w)]^n\} = (n-1)\{-\ln[(1 + q/k_s)e^{-\gamma_w \alpha z} - q/k_s]\}^n$$

$$1 + \{-\ln[(1 + q/k_s)e^{-\gamma_w \alpha z} - q/k_s]\}^n = (n-1)\{-\ln[(1 + q/k_s)e^{-\gamma_w \alpha z} - q/k_s]\}^n$$

$$\frac{1}{(n-2)} = \{-\ln[(1 + q/k_s)e^{-\gamma_w \alpha z} - q/k_s]\}^n$$

For the above equation to be true, or to have solutions for real number z, the left side of the equation has to be greater than zero, i.e.

$$n > 2 \tag{34}$$

Therefore, for n less than or equal to 2, the stress function (31) is a monotonic function of z. The regime of $0 \leq q/k_s$ and $n \leq 2$ represents the monotonic evaporation regime and is defined as Regime IV.

For $n>2$, Eq. (33) becomes

$$\frac{-1}{(n-2)^{1/n}} = \ln[(1 + q/k_s)e^{-\gamma_w \alpha z} - q/k_s]$$

$$e^{-1/(n-2)^{1/n}} = (1 + q/k_s)e^{-\gamma_w \alpha z} - q/k_s \tag{35}$$

$$\frac{e^{-1/(n-2)^{1/n}} + q/k_s}{1 + q/k_s} = e^{-\gamma_w \alpha z}$$

$$\ln\frac{e^{-1/(n-2)^{1/n}} + q/k_s}{1 + q/k_s} = -\gamma_w \alpha z_{\max} \tag{36}$$

The above equation may also be written conveniently as

$$\gamma_w \alpha z_{\max} = \ln \frac{1 + q/k_s}{e^{-1/(n-2)^{1/n}} + q/k_s} = \ln\left(\frac{1 + q/k_s}{1 + q/k_s e^{1/(n-2)^{1/n}}} e^{1/(n-2)^{1/n}} \right) \tag{37}$$

$$\gamma_w \alpha z_{\max} = \frac{1}{(n-2)^{1/n}} + \ln \frac{1 + q/k_s}{1 + \frac{q}{k_s} e^{1/(n-2)^{1/n}}} \tag{38}$$

Inequality (34) provides one constraint for the monotonic behavior of the stress function (31). Furthermore, for Eq. (36) to be mathematically equivalent to Eq. (35), we need

$$e^{-1/(n-2)^{1/n}} + q/k_s > 0$$
$$q/k_s > -e^{-1/(n-2)^{1/n}} \tag{39}$$

Inequality (39) provides another constraint for q/k_s as a function of parameter n. Regimes defined by Eqs. (34) and (39) can be subdivided into two regimes. For evaporation ($0 \leq q/k_s$ and $n > 2$), it is defined as Regime I. For small infiltration ($-e^{-(n-2)^{-1/n}} < q/k_s < 0$), it is defined as Regime II.

If inequality (39) is not satisfied, the stress function (31) will behave as a function of z monotonically. A limiting case is when Eq. (39) is becoming an equation, i.e.

$$q/k_s \to -e^{-1/(n-2)^{1/n}}$$
$$-q/k_s = e^{-1/(n-2)^{1/n}} \tag{40}$$

The above condition leads Eq. (36) becoming

$$\ln \frac{0}{q/k_s} = -\gamma_w \alpha z_{\max} \to -\infty$$

$$z_{\max} \to \infty$$

Eq. (40) provides a relationship between the flow ratio q/k_s and parameter n at the boundary of monotonic and maximum regime (Regime II) for the suction stress (31). For monotonic infiltration ($-1 < q/k_s \leq -e^{-(n-2)^{-1/n}}; q/k_s < 0;\ n > 1.0$) it is defined as Regime III.

Since Regimes I and II satisfy Eq. (39), there exists a maximum suction stress. Substituting Eq. (36) back into Eq. (31) in the following manner provides a way to find the maximum suction stress:

$$-\gamma_w \alpha z_{\max} = \ln \frac{e^{-1/(n-2)^{1/n}} + q/k_s}{1 + q/k_s}$$

$$e^{-\gamma_w \alpha z_{\max}} = \frac{e^{-1/(n-2)^{1/n}} + q/k_s}{1 + q/k_s}$$

$$(1 + q/k_s) e^{-\gamma_w \alpha z_{\max}} - q/k_s = e^{-1/(n-2)^{1/n}}$$

$$\ln[(1 + q/k_s) e^{-\gamma_w \alpha z_{\max}} - q/k_s] = \frac{-1}{(n-2)^{1/n}} = -\alpha(u_a - u_w)_{\max}$$

Therefore

$$\chi \frac{1}{(n-2)^{1/n}} = \chi \alpha (u_a - u_w)_{\max} = \frac{1}{(n-2)^{1/n}} \frac{1}{\{1 + [\alpha(u_a - u_w)]^n\}^{(n-1)/n}} \tag{41}$$

$$\chi \alpha (u_a - u_w)_{\max} = \frac{1}{(n-2)^{1/n}} \frac{1}{\{1 + [\alpha(u_a - u_w)]^n\}^{(n-1)/n}}$$
$$= \frac{1}{(n-2)^{1/n}} \frac{1}{\left[1 + \left(\frac{1}{(n-2)^{1/n}}\right)^n\right]^{(n-1)/n}}$$

$$\chi \alpha (u_a - u_w)_{\max} = \frac{1}{(n-2)^{1/n}} \frac{1}{\left[1 + \frac{1}{n-2}\right]^{(n-1)/n}}$$
$$= \frac{1}{(n-2)^{1/n}} \frac{1}{\left(\frac{n-1}{n-2}\right)^{(n-1)/n}}$$

$$\chi \alpha (u_a - u_w)_{\max} = \frac{1}{(n-2)^{1/n}} \frac{(n-2)^{(n-1)/n}}{(n-1)^{(n-1)/n}} = \frac{(n-2)^{(n-2)/n}}{(n-1)^{(n-1)/n}}$$

In summary, the maximum suction stress in Regimes I and II can be calculated analytically by Eq. (41), and its location can be calculated analytically by Eq. (36) or Eq. (37). If inequalities (34) and (39) are not satisfied, the stress function (31) behaves monotonically with the maximum suction stress followed by Eq. (31) and occurred at a distance of infinity or the boundary of the upper soil layer (Regime III for infiltration and Regime IV for evaporation).

References

Bao, C. G., Gong, B., and Zhan, L. (1998). "Properties of unsaturated soils and slope stability of expansive soil." Keynote Lecture, *in UNSAT 98, the 2nd Int. Conf. on Unsaturated Soils*, Beijing.

Bear, J. (1975). *Dynamics of fluids in porous media*, American Elsevier, New York.

Bishop, A. W. (1954). "The use of pore pressure coefficients in practice." *Geotechnique*, 4, 148–152.

Bishop, A. W. (1959). "The principle of effective stress." *Tek. Ukeblad*, 106(39), 859–563.

Blight, G. E. (1961). "Strength and consolidation characteristics of compacted soils." PhD dissertation, University of London, London.

Brooks, R. H., and Corey, A. T. (1964). "Hydraulic properties of porous media." *Colorado State University Hydrology Paper No. 3.*

Cho, G. C., and Santamarina, J. C. (2001). "Unsaturated particulate materials—Particle-level studies." *J. Geotech. Geoenviron. Eng.* 127(1), 84–96.

Donald, I. B. (1961). "The mechanical properties of saturated and partly saturated soils with special reference to negative pore water pressure." PhD dissertation, University of London, London.

Escario, V., and Juca, J. (1989). "Strength and deformation of partly saturated soils." *Proc., 12th Int. Conf. on Soil Mechanics and Foundation Engineering*, Vol. 3, 43–46, Rio de Janeiro.

Fisher, R. A. (1926). "On the capillary forces in an ideal soil." *J. Agric. Sci.*, 16, 492–505.

Fredlund, D. G., Ng, C. W. W., Rahardjo, H., and Leong, E. C. (2001). "Unsaturated soil mechanics: Who needs it?" *Geotech. News*, December. GeoSpec., Bi-Tech Publishing. Vancouver, B.C., Canada, 43–45

Fredlund, D. G., and Xing, A. (1994). "Equations for the soil-water characteristic curve." *Can. Geotech. J.*, 31, 521–532.

Gardner, W. R. (1958). "Steady state solutions of the unsaturated moisture flow equation with application to evaporation from a water table," *Soil Sci.*, 85, 228–232.

Iwata, S., and Tabuchi, T. (1988). *Soil water interaction: Mechanisms and applications*, Marcel Dekker, New York.
Khalili, N., and Khabbaz, M. H. (1998). "A unique relationship for the determination of the shear strength of unsaturated soils," *Geotechnique*, 48(5), 681–687.
Krahn, J., Fredlund, D. G., and Klassen, M. J. (1989). "Effect of soil suction on slope stability at Notch Hill." *Can. Geotech. J.*, 26, 269–278.
Marshall, T. J., and Holmes, J. W. (1988). *Soil Physics*, 2nd ed., Cambridge University Press, Cambridge, U.K.
Oberg, A., and Sallfors, G. (1997). "Determination of shear strength parameters of unsaturated silts and sands based on the water retention curve." *Geotech. Test. J.*, 20(1), 40–48.
Phillips, J. R. (1987). "The quasi-linear analysis, the scattering analog and other aspects of infiltration and seepage." *Infiltration development and application*, Y. S. Fok, ed., Water Resources Research Center, Univ. of Hawaii, Hawaii, 1–27.
Rahardjo, H., and Leong, E. C. (1997). "Soil-water characteristic curves and flux boundary problems." *Proc., Unsaturated Soil Engineering Practice*, GSP No. 68, S. L. Houston and D. G. Fredlund, eds., ASCE, 89–112.
Singh, V. P. (1997). *Kinematic wave modeling in water resources*, Wiley, New York.
Sparks, A. D. W. (1961). "Partially saturated soils-classification; compressibility of the fluid phase; and the stress equations." MSc thesis, Univ. of the Witwatersrand.
Stephens, D. B. (1995). *Vadose zone hydrology*, CRC, Boca Raton, Fla.
Terzaghi, K. (1925). *Erdbaumechanik*, Vienna, Franz Deuticke.
Terzaghi, K. (1943). *Theoretical soil mechanics*, Wiley, New York.
Totoev, Y. Z., and Kleeman, P. W. (1998). "An infiltration model to predict suction changes in the soil profile." *Water Resour. Res.*, 34(7), 1617–1622.
Vanapalli, S. K., and Fredlund, D. G. (2000). "Comparison of different procedure to predict unsaturated soil shear strength." *Proc., Advances in unsaturated geotechnics*, GSP No. 99, C. D. Shackelford, S. L. Houston, and N. Y. Chang, eds., ASCE, Reston, Va., 195–209.
Vanapalli, S. K., Fredlund, D. G., Pufahl, D. E., and Clifton, A. W. (1996). "Model for the prediction of shear strength with respect to soil suction." *Can. Geotech. J.*, 33, 379–392.
Van Genuchten, M. T. (1980). "A closed form equation for predicting the hydraulic conductivity of unsaturated soils." *Soil Sci. Soc. Am. J.*, 44, 892–898.
Wilson, G. W. (1997). "Surface flux boundary modeling for unsaturated soils." *Proc., Unsaturated Soil Engineering Practice*, Geotechnical Special Publication No. 68, ASCE.
Yeh, T.-C. J. (1989). "One-dimensional steady state infiltration in heterogeneous soils." *Water Resour. Res.*, 25(10), 2149–2158.